Modeling the influence of thermo-mechanical crack opening and closure on rock stiffness

C. Zhu[1] and C. Arson[2]

[1]Geosystems Group, School of Civil and Environmental Engineering, Georgia Institute of Technology; 790 Atlantic Drive, Atlanta, GA 30332-0355; (678)-761-2835; chengzhu@gatech.edu;
[2]Geosystems Group, School of Civil and Environmental Engineering, Georgia Institute of Technology; 790 Atlantic Drive, Atlanta, GA 30332-0355; (404)-385-0143 chloe.arson@ce.gatech.edu

ABSTRACT

A thermodynamic framework is proposed to model the effect of mechanical stress and temperature on crack opening and closure in rocks. The model is based on Continuum Damage Mechanics with damage defined as the second-order crack density tensor. The free energy of damaged rock is expressed as a function of deformation, temperature and damage. The damage criterion controls mode I crack propagation, captures temperature-induced decrease of rock toughness, and accounts for the increase of energy release rate necessary to propagate cracks induced by damage. Crack closure is modeled through unilateral effects produced on rock stiffness. Simulations show that: (1) under anisotropic mechanical boundary conditions, crack closure occurs during cooling, (2) the thermo-mechanical strain energy necessary to close cracks during cooling is larger than the strain energy needed to close the cracks by mechanical compression. Parametric study highlights the thermo-mechanical stress redistributions occurring during closure. The proposed framework is expected to bring new insights in the design and reliability assessment of geotechnical reservoirs and repositories.

1. Introduction

Crack initiation and propagation are important issues in the design of geotechnical reservoirs and repositories. Thermo-mechanical stresses can originate various micro-structure changes, such as void nucleation, mode I crack opening, and linkage of shear cracks. In Continuum Damage Mechanics (CDM), the strain energy loss due to crack propagation is used to compute damaged stiffness and deformation. This approach is purely energetic and does not require a geometric description of the crack pattern. The second-order crack density tensor defined by Kachanov (1992) is particularly well-suited to evaluate damaged elastic properties of a solid with non-interacting cracks. Closure of tensile cracks allows recovery of compressive strength rather than tensile strength, which is known as unilateral effects. A way of formulating the unilateral condition for active/passive damage has been proposed by Chaboche (1993). Halm & Dragon (1998) extended the anisotropic mechanical model of crack closure to account for frictional sliding at crack faces. Most thermo-mechanical damage models for rock are based on crack-induced volumetric cracking, captured by a "dilatancy boundary", like in salt rock (Hunsche and Hampel, 1999; Hou, 2003). This class of models (see also Chan *et al.*, 2001) do not capture stiffness changes and could not predict damage-induced anisotropy in a sedimentary rock. In the thermo-mechanical damage model proposed by Zhou *et al.* (2011), a scalar damage variable is injected in plastic and viscoplastic hardening laws and is used to model stiffness degradation. Irreversible deformation is considered rate-dependent, but damage is considered rate-independent. In general, two flow rules are needed to close the model formulation: the rate of inelastic deformation and the rate of damage (affecting the stiffness tensor).

In this research, a thermodynamic framework based on CDM is proposed to model the effects of thermo-mechanical coupled stress on crack opening and closure in rock. The thermodynamic framework is presented in Section 2. Emphasis is put on the assumptions made in the model to couple the effects of internal tensile stress and temperature. Section 3 presents simulations of load paths including mechanical crack opening, mechanical crack closure, and thermo-mechanical crack closure.

2. Outline of the Model of Thermo-Mechanical Crack Opening and Closure

2.1 Thermo-mechanical free energy of the damaged rock skeleton

A hyper-elastic framework is adopted (Houlsby and Puzrin, 2006), i.e. it is assumed that the elasticity tensor derives from an energy potential. Stress is conjugate to elastic deformation. The damage variable ($\mathbf{\Omega}$) is defined as the second-order crack density tensor (Kachanov, 1992). Assuming that rock has a linear thermo-elastic behavior in the absence of damage, the free energy for rock solid skeleton is sought in the form of a polynomial of elastic deformation and temperature. Taking Halm & Dragon's (1998) rock mechanical damage model as a reference, it is assumed that the free energy should be a linear function of damage. Rock skeleton free energy is expressed as:

$$\Psi_S(\varepsilon^E, \tau, \mathbf{\Omega}) = \frac{1}{2}\varepsilon^E : \mathbf{D}(\mathbf{\Omega}) : \varepsilon^E + g\mathbf{\Omega} : \varepsilon - \frac{1}{2\tau_0}C(\mathbf{\Omega})\tau^2 - \tau K(\mathbf{\Omega}) : \varepsilon^E \tag{1}$$

where the damaged elastic strain energy is expressed in the same way as in Halm & Dragon's model, but in terms of elastic deformation (ε^E) instead of total deformation (ε) in order to stay in the framework of hyper-elasticity:

$$\begin{aligned} \frac{1}{2}\varepsilon^E : \mathbf{D}(\mathbf{\Omega}) : \varepsilon^E &= \frac{1}{2}\lambda(tr\varepsilon^E)^2 + \mu\, tr(\varepsilon^E \cdot \varepsilon^E) \\ &\quad + \alpha\, tr\varepsilon^E\, tr(\varepsilon^E \cdot \mathbf{\Omega}) + 2\beta\, tr(\varepsilon^E \cdot \varepsilon^E \cdot \mathbf{\Omega}) \end{aligned} \tag{2}$$

in which $\mathbf{D}(\mathbf{\Omega})$ is the damaged stiffness tensor. The term $g\mathbf{\Omega} : \varepsilon$ is kept unchanged from Halm & Dragon's formulation, and represents the energy that needs to be released to close residual cracks (i.e., cracks that remain open after release of tensile loading). The two last terms of the free energy ($-\frac{1}{2\tau_0}C(\mathbf{\Omega})\tau^2 - \tau K(\mathbf{\Omega}) : \varepsilon^E$) are the classical linear thermo-elastic energy potentials. λ and μ are Lamé coefficients, g, α, and β are damaged material parameters, τ_0 is the initial temperature, τ is the temperature change, $C(\mathbf{\Omega})$ is the damaged heat capacity, $K(\mathbf{\Omega})$ is the product of the damaged bulk modulus ($k(\mathbf{\Omega})$) by the solid skeleton thermal expansion coefficient (α_T). Cracks are assumed to reduce the area of effective material surfaces that can resist internal forces. However, in the undamaged part of the bulk (i.e. outside the cracks), solid properties are unchanged. That is the reason why the thermal expansion coefficient α_T is assumed to remain constant, while the bulk modulus $k(\mathbf{\Omega})$ depends on damage.

Conjugation relationships provide the expressions of stress and damage-driving force, with the damage-driving force further decomposed into two parts:

$$\sigma = \frac{\partial \Psi_S(\varepsilon^E, \tau, \mathbf{\Omega})}{\partial \varepsilon^E} = \mathbf{D}(\mathbf{\Omega}) : \varepsilon^E + g\mathbf{\Omega} - K(\mathbf{\Omega})\tau \tag{3}$$

$$\mathbf{Y} = -\frac{\partial \Psi_S(\varepsilon^E, \tau, \mathbf{\Omega})}{\partial \mathbf{\Omega}} = \mathbf{Y_1} + \mathbf{Y_2} \tag{4}$$

$$\mathbf{Y_1} = -g\varepsilon - \alpha(tr\varepsilon)\varepsilon - 2\beta(\varepsilon \cdot \varepsilon) \tag{5}$$

$$\mathbf{Y_2} = \frac{1}{2\tau_0}\frac{\partial C(\mathbf{\Omega})}{\partial \mathbf{\Omega}}\tau^2 + \tau\frac{\partial K(\mathbf{\Omega})}{\partial \mathbf{\Omega}} : \varepsilon^E \tag{6}$$

2.2 Incremental constitutive relationships

Stress evolution can be derived from Eq. (3):

$$d\sigma = \mathbf{D}(\mathbf{\Omega}) : d\varepsilon^E + (\frac{\partial D(\mathbf{\Omega})}{\partial \mathbf{\Omega}} : \varepsilon^E) : d\mathbf{\Omega} + gd\mathbf{\Omega} - K(\mathbf{\Omega})d\tau - (\frac{\partial K(\mathbf{\Omega})}{\partial \mathbf{\Omega}}d\mathbf{\Omega})\tau \tag{7}$$

The total deformation tensor is split into three components (Abu Al-Rub and Voyiadjis, 2003), as shown in Fig. 1:

$$\varepsilon = \varepsilon^e + \varepsilon^{ed} + \varepsilon^{id} = \varepsilon^E + \varepsilon^{id} \tag{8}$$

in which ε^e is the purely elastic deformation recoverable by unloading in the absence of damage. ε^{ed} is the additional elastic deformation associated with the change of stiffness due to damage. ε^{id} is the irreversible deformation induced by damage, representing residual cracks that remain open after unloading. Total elastic deformation is the sum of purely elastic and damage-induced elastic deformation: $\varepsilon^E = \varepsilon^e + \varepsilon^{ed}$. The increment of elastic deformation is split into a mechanical and a thermal component:

$$d\varepsilon^E = d\varepsilon^{EM} + d\varepsilon^{ET} \tag{9}$$

The damage criterion is expressed as the difference between the norm of an energy re-

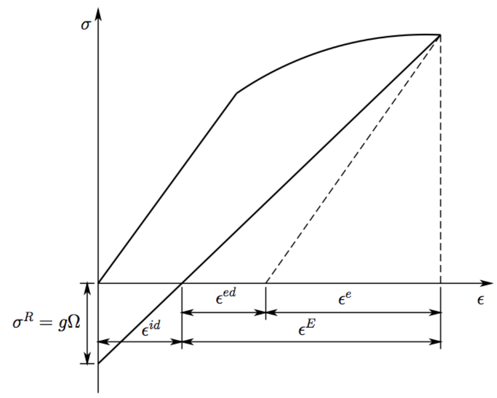

Figure 1: Decomposition of deformation for a typical loading and unloading cycle.

lease rate and an energy threshold. The latter depends on hardening variables. Only certain components of the thermodynamic variable conjugate to damage ($\mathbf{Y}$) is expected to contribute to crack propagation, mainly: mechanical and thermal tensile stress maintaining cracks open after unloading. In addition, rock toughness is expected to decrease with a temperature increase. The purpose of the following development is to define a function for the energy release rate involved in the damage criterion, according to the physical trends explained above. The damage driving force component $\mathbf{Y_1}$ (Eq. (5)) is decomposed into:

$$\mathbf{Y_1} = \mathbf{Y_{1a}} + \mathbf{Y_{1b}}, \quad \mathbf{Y_{1a}} = -g\varepsilon, \quad \mathbf{Y_{1b}} = -\alpha(tr\varepsilon)\varepsilon - 2\beta(\varepsilon \cdot \varepsilon), \tag{10}$$

$$\mathbf{Y_{1a}}^+ = -g\varepsilon^+, \quad \mathbf{Y_{1a}}^- = -g(\varepsilon - \varepsilon^+) \tag{11}$$

In mode I crack propagation, it is assumed that $\mathbf{Y_{1a}}^+$ will be the dominating damage-driving force. Note that $\mathbf{Y_{1a}}^+$ accounts for tensile deformation due to internal tensile forces induced by mechanical stress or temperature increase (Eq. (9)). $\mathbf{Y_2}$ (Eq. (6)) accounts for the change of rock properties due to temperature changes ($\mathbf{Y_2} = \mathbf{0}$ in a purely mechanical damage model). A quick dimensional analysis indicates that the term $\frac{1}{2\tau_0}\frac{\partial C(\mathbf{\Omega})}{\partial \mathbf{\Omega}}\tau^2$ can be neglected ($\frac{\partial C(\mathbf{\Omega})}{\partial \mathbf{\Omega}} \ll \frac{\partial K(\mathbf{\Omega})}{\partial \mathbf{\Omega}}$). According to the definition of the bulk modulus, and according to Eqs. (2) and (6), $\mathbf{Y_2}$ should be proportional to $\alpha_T(\alpha + 2\beta)\tau$, and should vary like a polynomial of order one in elastic deformation. In addition, inter-particle distance in rock increases with temperature. At higher temperatures, it requires more energy to increase the distance between rock crystals by propagating a crack. To counter-act the tensile damage-driving force $\mathbf{Y_{1a}}^+$, the following thermal damage-driving force can be defined:

$$\mathbf{Y_2}^d = A \cdot \tau \cdot \alpha_T(\alpha + 2\beta)tr(\varepsilon^{E+}) \tag{12}$$

where ε^{E+} is the tensile elastic deformation, which indicates the increase of inter-particle distance at high temperature. A is a proportionality constant. As a conclusion, the total damage-driving force retained in the proposed thermo-mechanical damage model (noted $\mathbf{Y_d}^+$) is defined as:

$$\mathbf{Y_d}^+ = \mathbf{Y_{1a}}^+ + \mathbf{Y_2}^d = -g\varepsilon^+ + A \cdot \tau \cdot \alpha_T(\alpha + 2\beta)tr(\varepsilon^{E+}) \tag{13}$$

The damage criterion is written in the form of "norm of force - threshold":

$$f_d(\mathbf{Y_d}^+, \mathbf{\Omega}) = \sqrt{\frac{1}{2}\mathbf{Y_d}^+ : \mathbf{Y_d}^+} - (C_0 + C_1\mathbf{\Omega}) \tag{14}$$

in which C_0 is the initial damage threshold which is necessary to trigger damage, and C_1 is a parameter which controls crack growth with cumulated damage. Using the consistency conditions (i.e., $f_d = 0$ and $\dot{f}_d = 0$), the increments of Lagrange multiplier and damage are calculated as:

$$d\lambda_d = -\frac{\frac{\partial f_d}{\partial \mathbf{Y_d}^+} : d\mathbf{Y_d}^+}{\frac{\partial f_d}{\partial \mathbf{\Omega}} : \frac{\partial f_d}{\partial \mathbf{Y_d}^+}} = \frac{\mathbf{Y_d}^+ : d\mathbf{Y_d}^+}{(C_1\delta) : \mathbf{Y_d}^+} \tag{15}$$

$$d\mathbf{\Omega} = d\lambda_d \frac{\partial f_d(\mathbf{Y_d}^+, \mathbf{\Omega})}{\partial \mathbf{Y_d}^+} = \frac{[\frac{\mathbf{Y_d}^+}{\sqrt{2\mathbf{Y_d}^+ : \mathbf{Y_d}^+}}] : d\mathbf{Y_d}^+}{(C_1\delta) : [\frac{\mathbf{Y_d}^+}{\sqrt{2\mathbf{Y_d}^+ : \mathbf{Y_d}^+}}]} [\frac{\mathbf{Y_d}^+}{\sqrt{2\mathbf{Y_d}^+ : \mathbf{Y_d}^+}}] \tag{16}$$

2.3 Unilateral effects of crack closure on damaged stiffness

The recovery of compression strength by the closure of tensile cracks is known as unilateral effects in Continuum Damage Mechanics. In general, the expression of unilateral recovery of stiffness induced by crack closure is (Chaboche, 1993):

$$D_{eff}(\mathbf{\Omega}) = D(\mathbf{\Omega}) + \eta \sum_{k=1}^{3} H(-tr(P_i : \varepsilon))P_i : (D_0 - D(\mathbf{\Omega})) : P_i \tag{17}$$

in which $D_{eff}(\mathbf{\Omega})$ is the partially recovered stiffness tensor and $\mathbf{P_i}$ is the fourth order projection tensor (projection in crack planes normal to direction i). H is the Heaviside function. η is a parameter the indicates the degree of maximum stiffness recovery ($0 < \eta \leq 1$). In the following simulations, it is assumed that stiffness is fully recovered ($\eta = 1$) under compression loading when cracks are closed.

3. Numerical Study of Thermo-Mechanical Crack Closure

3.1 Unilateral effects of crack closure on damaged stiffness

An algorithm has been written in MATLAB to simulate crack opening and closure under axis-symmetric uniaxial loading, with the thermo-mechanical (TM) damage model presented above. Mechanical and damage parameters calibrated by Halm & Dragon (1998) for Fontainebleau sandstone are used. The only thermal parameter required is the thermal expansion coefficient, which is given a standard value for rock materials (Table 1).

The thermo-mechanical test simulated consists of a uniaxial tension phase, followed by a compression phase to release tensile stress. After this second phase, elastic damage-induced deformation is recovered, but residual cracks remain open: $\varepsilon = \varepsilon^{id}$. Two cases are simulated for the third loading stage:

- a decrease of temperature under the constraint that axial deformation is zero,
- a purely mechanical axial compression (at constant temperature).

Table 1: Material parameters used in the thermo-mechanical simulations.

λ (Pa)	μ (Pa)	α (Pa)	β (Pa)
2.63×10^{10}	1.75×10^{10}	1.9×10^{9}	-2.4×10^{10}
g (Pa)	C_0 (Pa)	C_1 (Pa)	$\alpha_T(K^{-1})$
1.1×10^{8}	1000	5.5×10^{5}	-1×10^{-5}

The present analysis focuses on opening and closure of one family of cracks perpendicular to the axis of loading. That is why compression in the third loading phase is kept below sandstone compression strength (to avoid the formation of axial cracks). The principle of the test is explained in Table 2. Soil mechanics sign convention is adopted (i.e. compression is counted positive).

Table 2: Loading phases simulated in the study of thermo-mechanical crack closure.

<table>
<tr><th>(1) Uniaxial tension</th><th>(2) Compression: release of tensile stress</th></tr>
<tr><td>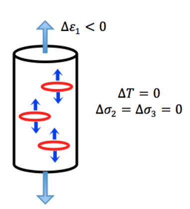
</td><td>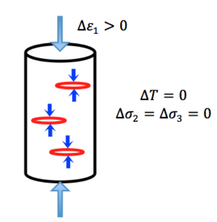
</td></tr>
<tr><td>OA (elastic) - AB (damage)</td><td>BC ("elastic" crack closure)</td></tr>
<tr><th colspan="2">(3) Further compression: full closure and unilateral effects</th></tr>
<tr><th>(a) Compression induced by cooling</th><th>(b) Mechanical compression</th></tr>
<tr><td>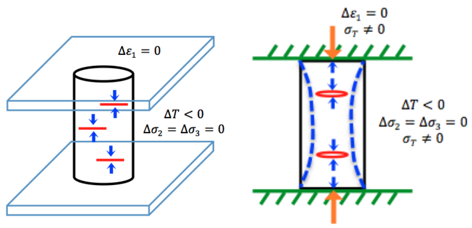
</td><td>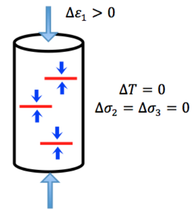
</td></tr>
<tr><td colspan="2">CD (closure of residual cracks) - DE (unilateral effects)</td></tr>
</table>

(1) Uniaxial tension (OA-AB)

The sample is loaded by increasing the axial tensile strain with a constant strain rate ($\Delta\varepsilon_1$). Temperature and lateral stress are kept constant ($\Delta\sigma_2 = \Delta\sigma_3 = 0$, $\Delta T = 0$). Crack planes perpendicular to the axis are produced due to the tensile stress.

(2) Compression: release of tensile stress (BC)
The sample is unloaded in order to release the tensile stresses completely. The unloading process is elastic (linear stress/strain plot), and only the elastic part of crack-induced deformation is compensated (at the end of this loading phase: $\varepsilon^{ed} = 0$, but $\varepsilon^{id} \neq 0$).

(3) Further compression: full closure and unilateral effects (CD-DE)
Residual cracks are expected to close either by cooling or by mechanical compression (Table 2). During cooling (3a), mechanical boundary conditions are applied: the sample is free to contract laterally, but not axially ($\Delta\epsilon_1 = 0,\ \Delta\sigma_2 = \Delta\sigma_3 = 0$). Consequently, internal tensile forces develop in the undamaged part of the sample (i.e., outside the cracks). In virtue of the principle of action and reaction, cracks close due to internal compression forces that act at crack faces (3a, Table 2). In the mechanical compression phase (3b), further compressive strain is applied at a constant rate ($\Delta\varepsilon_1$) under constant lateral stress ($\Delta\sigma_2 = \Delta\sigma_3 = 0$).

3.2 Thermo-mechanical (TM) crack closure

During the first loading phase, an axial tensile strain of $\varepsilon_1 = -0.0011$ is applied incrementally (at constant rate). Rock tensile strength is relatively low, so that damage starts to develop quickly after the tensile load is applied. Correspondingly, the stress-strain curve is linear on a very short interval (OA, Fig. 2.a), which is followed by a non-linear response (AB, Fig. 2.a) associated to the development of damage (Fig. 3.b). During the stress release phase, the sample is unloaded elastically, and elastic deformation induced by damage (ε^{ed}) is recovered (BC, Fig. 2.a). During this phase, neither the damage-driving force or damage evolve (BC, Fig. 3).

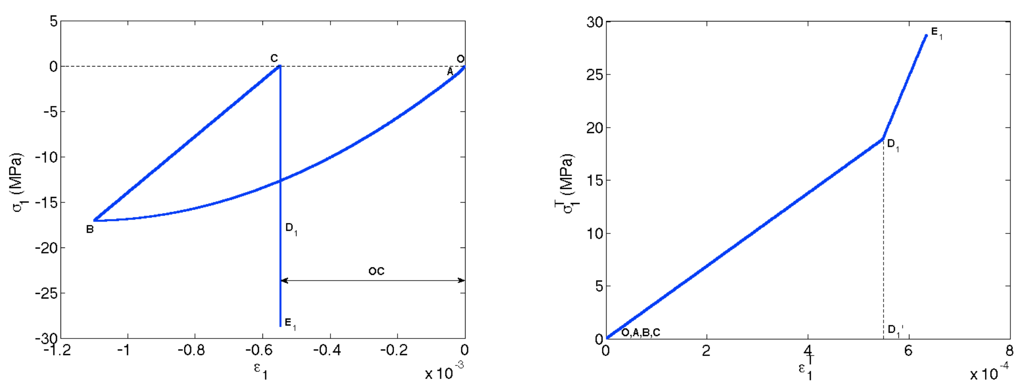

(a) (b)

Figure 2: Stress-strain diagrams for TM crack closure. (a) Total stress vs. axial deformation. (b) Thermal stress vs. thermal strain. (length of OC equals to length of OD_1')

Cooling is simulated with $\Delta T = -300K$. Axial deformation is fixed ($\varepsilon_1 = 0$). In virtue of action/reaction principles, compressive thermal stresses apply to crack faces (CD_1, Fig. 2.b). The slope of the thermal stress/thermal strain diagram depends on the bulk modulus. When cracks are completely closed, unilateral effects induce an increase of stiffness, thus, an increase of bulk modulus (slope D_1E_1, Fig. 2.b). During the cooling phase, lateral deformation is a contraction, and the sum of thermal and mechanical axial deformation is zero, so that the damage driving force defined in Eq. (13) remains constant. As a result, damage does not increase (C-D_1-E_1, Fig. 3).

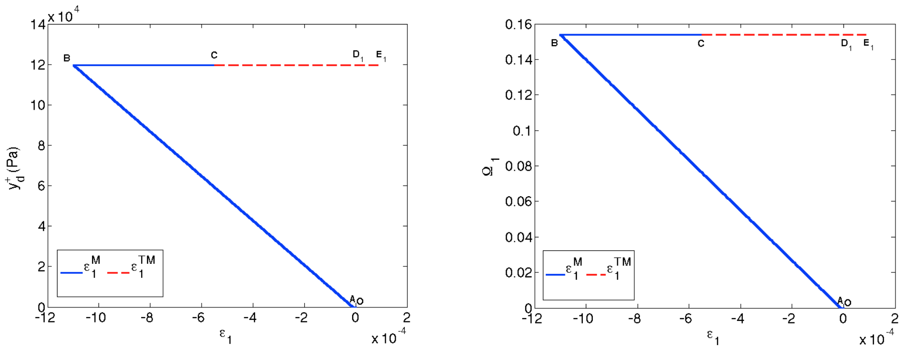

(a) (b)

Figure 3: Simulation of thermo-mechanical crack closure. (a) Axial damage-driving force (direction 1). (b) Damage variable (direction 1)

3.3 Comparison of thermo-mechanical (TM) to purely mechanical (M) crack closure

The same extension and stress release phases as Section 3.2 are simulated again, followed by a purely mechanical compression phase (3b. in Table 2). As long as total deformation is negative (tension), the slope (CD_2) of the stress/strain diagram in stage 3 is the same as in stage 2 (BC) (Fig. 4). Once residual cracks are completely closed (i.e., $\varepsilon = 0$), deformation becomes positive (compression), and unilateral effects induce mechanical stiffness recovery in compression. As a result, the slope of the stress/strain diagram becomes steeper (D_2E_2 in Fig. 4) and is actually equal to the slope of OA.

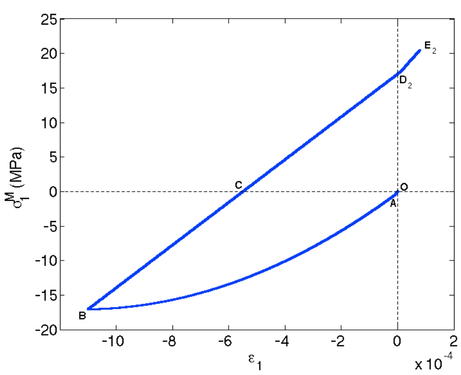

Figure 4: Stress-strain diagram (crack closure by purely mechanical loading)

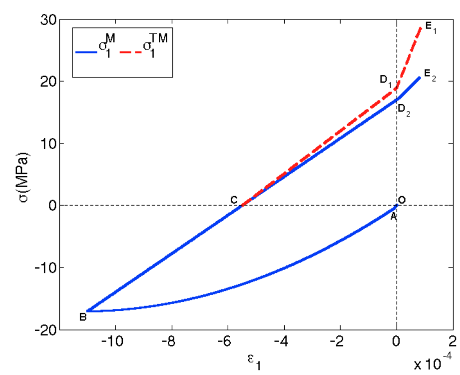

Figure 5: Stress-strain diagram (TM crack closure vs. M crack closure)

The combined plots shown in Fig. 5 reveal that both thermo-mechanical and purely mechanical processes can completely close the residual cracks. The relative position of the stress/strain diagrams shows that the strain energy needed to close residual cracks by mechanical compression is less than the energy associated to the equivalent thermal deformation developed during cooling. Mechanical compression is more work-efficient than cooling to close the cracks.

3.4 Parametric study on the initial state of damage

A parametric study is conducted in order to explore the effect of initial damage, i.e. the effect of damage generated after the tensile loading phase. Axial tension is simulated for four values of maximum deformation: -0.0003, -0.0006, -0.0009, and -0.0011. As could be expected, higher initial damage result in smaller stiffness, which is illustrated by the decrease of the slope of the mechanical unloading curve (BC) as axial deformation is increased (Fig. 6). The stress needed to close completely the residual cracks increases with the tensile loading applied in stage 1.

When "residual cracks" are closed by cooling-induced compression, it is found (Fig. 7) that the temperature change needed to close residual cracks increases with the tensile loading applied in stage 1 (i.e. with initial damage). The required temperature drop increases (in absolute value) from -58K ($\varepsilon_1 = -0.0003$), -120K ($\varepsilon_1 = -0.0006$), -201K ($\varepsilon_1 = -0.0009$) to -274K ($\varepsilon_1 = -0.0011$). Higher initial damage result in smaller bulk modulus, which is illustrated by the decrease of the slopes of obtained during stress release and cooling (Fig. 7).

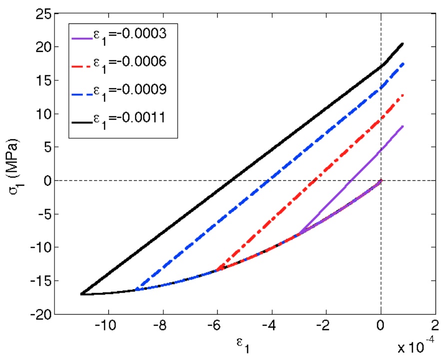

Figure 6: Stress-strain diagrams for various initial states of damage (crack closure by purely mechanical loading).

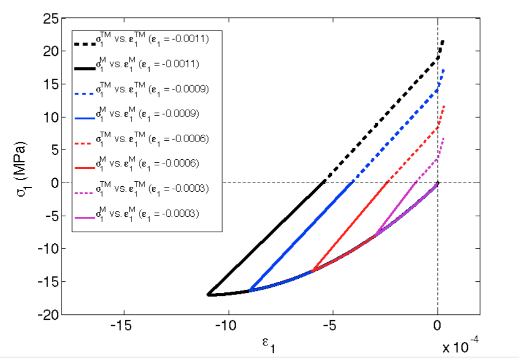

Figure 7: Stress-strain diagrams for various initial states of damage (crack closure by cooling).

4. Conclusion

A thermodynamic framework is proposed to model the effect of mechanical stress and temperature on crack opening and closure in rock. The model is based on CDM, with damage defined as the second-order crack density tensor. Halm & Dragon's model (1998) is used as a basis to postulate the free energy, in the form of a polynomial of deformation, temperature and damage. Thermo-elastic energy potentials are made dependent on damage - by assuming that in addition to the bulk modulus, heat capacity is affected by damage. Conjugation relationships indicate that stress and damage-driving force depend on internal variables (e.g., damage) and external variables (e.g., strain and temperature). The energy release rate controlling damage propagation is a modified damage driving force. The damage criterion controls mode I crack propagation, captures temperature-induced decrease of rock toughness, and accounts for the increase of energy release rate necessary to propagate cracks in a damaged medium. Crack closure is modeled through unilateral effects produced on rock stiffness.

Uniaxial tension tests followed by unloading and further compression have been simulated using MATLAB. The degradation of stiffness due to tensile stress and recovery of stiffness due to unilateral effects are well captured. Simulation of the confined cooling phase also illustrates the capability of the model to predict crack closure induced by coupled thermo-mechanical stresses. Parametric studies highlight the TM stress redistributions occurring during closure. Further work will be dedicated to model validation and calibration against published experimental data, to the simulation of crack opening under compression after closure of tension-induced cracks, and to the modeling of the coupled effects of crack opening, closure and healing.

REFERENCES

Abu Al-Rub, R. K. and Voyiadjis, G. Z. (2003). "On the coupling of anisotropic damage and plasticity models for ductile materials." *International Journal for Solids and Structures*, 40(11), 2611-2643.

Chaboche, J. L. (1993). "Development of continuum damage mechanics for elastic solids sustaining anisotropic and unilateral damage." *International Journal of Damage Mechanics*, 2(4), 311-329.

Chan, K. S., Bodner, S. R., and Munson, D. E. (2001). "Permeability of WIPP salt during damage evolution and healing." *International Journal of Damage Mechanics*, 10(4), 347-375.

Halm, D. and Dragon, A. (1998). "An anisotropic model of damage and frictional sliding for brittle materials." *Eur. J. Mech. A/Solids*, 17(3), 439-460.

Hou, Z. (2003). "Mechanical and hydraulic behavior of rock salt in the excavation disturbed zone around underground facilities." *International Journal of Rock Mechanics and Mining Sciences*, 40(5), 725-738.

Houlsby, G. T., and Puzrin, A. M. (2006). *Principles of Hyperplasticity. An Approach to Plasticity Theory Based on Thermodynamic Principles.* Springer, London.

Hunsche, U. and Hampel, A. (1999). "Rock salt the mechanical properties of the host rock material for a radioactive waste repository." *Engineering Geology*, 52(3), 271-291.

Kachanov, M. (1992). "Effective elastic properties of cracked solids: critical review of some basic concepts." *Appl. Mech. Rev. (ASME)*, 45(8), 304-335.

Zhou, H., Hu, D., Zhang, F., and Shao, J. (2011). "A thermo-plastic/viscoplastic damage model for geomaterials." *Acta Mech Solida Sinica*, 24(3), 195-208.